

A pulsating early-B type star with an extremely strong magnetic field: Characterizing CPD -62° 2124

S. Hubrig^{1*}, A. F. Kholtygin², I. Ilyin¹, M. Schöller³, S. P. Järvinen¹

¹ Leibniz-Institut für Astrophysik Potsdam (AIP), An der Sternwarte 16, 14482 Potsdam, Germany

² Saint-Petersburg State University, Universitetskij pr. 28, Saint-Petersburg 198504, Russia

³ European Southern Observatory, Karl-Schwarzschild-Str. 2, 85748 Garching, Germany

Accepted Received; in original form

ABSTRACT

A strong longitudinal magnetic field of the order of 5.2 kG was recently detected in CPD -62° 2124 in the framework of the BOB collaboration. Our spectropolarimetric monitoring of this star with FORS 2 at the VLT revealed the presence of a huge magnetic field dominated by a dipolar component with a polar strength between 32.5 and 35.7 kG. Such an extraordinary strong magnetic field strength was not previously detected in any massive early-B type star. Although being in an advanced evolutionary state, CPD -62° 2124 rotates fast with $v_{\text{eq}} \geq 176 \text{ km s}^{-1}$ over the period $P_{\text{rot}} = 1.45031 \pm 0.00002 \text{ d}$. An analysis of the spectral variability of CPD -62° 2124 on different time scales shows, apart from the rotational modulation of the line profiles, also distinct changes in shape and position of line profiles taking place on time-scales corresponding to the duration of the sub-exposure sequences. This short-term variability can probably be attributed to β Cep like pulsations. The rotational variability pattern of hydrogen and metal lines exhibits a similar behaviour while the He lines vary opposite to all other elements studied, indicating a different elemental surface distribution.

Key words: stars: early type — stars: individual: CPD -62° 2124 — stars: magnetic field — stars: chemically peculiar — stars: pulsation — techniques: polarimetric

1 INTRODUCTION

The detection of a very strong magnetic field of the order of 5.2 kG in the chemically peculiar early-B type star CPD -62° 2124 was previously reported by Castro et al. (2017) who used one spectropolarimetric observation with the High Accuracy Radial velocity Planet Searcher (HARPSpol; Snik et al. 2011) attached to the ESO 3.6m telescope on La Silla and one observation with the FOcal Reducer low dispersion Spectrograph (FORS 2; Appenzeller et al. 1998) mounted on the 8 m Antu telescope of the VLT. Assuming a certain dipolar magnetic field geometry to estimate the dipolar magnetic field strength of about 18.3 kG, Castro et al. (2017) suggested that no other early-B type star is known to host a magnetic field with a comparable strength. Moreover, the study of the stellar parameters, using a comparison with stellar evolutionary tracks, indicated that CPD -62° 2124 is largely evolved from the zero-age main sequence with a fractional main-sequence lifetime of about 60%.

Our recent monitoring of this star employing multi-epoch FORS 2 spectropolarimetric observations distributed over about two and a half months revealed that the magnetic field is even stronger than previously anticipated, with a maximum longitudinal magnetic field strength of up to 6.75 kG, depending on the assumed

stellar radius. In the following sections, we present the results of our magnetic field measurements, the search for a magnetic field periodicity, and discuss the detected spectral variability, including pulsational variability.

2 OBSERVATIONS AND MAGNETIC FIELD MEASUREMENTS

Sixteen FORS 2 spectropolarimetric observations of CPD -62° 2124 were obtained from 2016 March 12 to May 24. The FORS 2 multi-mode instrument is equipped with polarisation analysing optics comprising super-achromatic half-wave and quarter-wave phase retarder plates, and a Wollaston prism with a beam divergence of $22''$ in standard resolution mode. We used the GRISM 600B and the narrowest available slit width of 0.4 to obtain a spectral resolving power of $R \sim 2000$. The observed spectral range from 3250 to 6215 Å includes all Balmer lines, apart from $H\alpha$, and numerous helium lines. For the observations, we used a non-standard readout mode with low gain (200kHz, 1×1 , low), which provides a broader dynamic range, hence allowing us to reach a higher signal-to-noise ratio (SNR) in the individual spectra. The exposure time for each subexposure accounted for 7 min. A detailed description of the assessment of longitudinal magnetic field measurements using FORS 1/2 spectropolarimetric

* E-mail: shubrig@aip.de

Table 1. Logbook of the FORS2 polarimetric observations of CPD -62° 2124, including the modified Julian date of mid-exposure followed by the achieved signal-to-noise ratio in the Stokes I spectra around 5000 \AA , and the measurements of the mean longitudinal magnetic field using the Monte Carlo bootstrapping test, only for the hydrogen lines and for all lines. In the last columns, we present the results of our measurements using the null spectra for the set of all lines and the phases calculated relative to a zero phase corresponding to a positive field extremum at MJD57300.3407. All quoted errors are 1σ uncertainties.

MJD	SNR	$\langle B_z \rangle_{\text{hyd}}$ [G]	$\langle B_z \rangle_{\text{all}}$ [G]	$\langle B_z \rangle_{\text{N}}$ [G]	Phase
57099.2449	1846	4636 \pm 128	4419 \pm 87	5 \pm 63	0.343
57460.1011	1092	5601 \pm 239	5508 \pm 182	-8 \pm 150	0.156
57461.0599	1308	6516 \pm 280	6274 \pm 159	-35 \pm 100	0.817
57462.0660	1423	3965 \pm 140	3737 \pm 98	25 \pm 88	0.511
57463.0650	1306	5637 \pm 288	5704 \pm 143	1 \pm 84	0.200
57465.2482	1401	5144 \pm 191	4671 \pm 173	143 \pm 110	0.705
57474.0863	1013	6753 \pm 429	5645 \pm 214	-44 \pm 112	0.799
57478.2042	1733	4468 \pm 145	4122 \pm 113	-18 \pm 71	0.638
57478.2560	1787	4269 \pm 180	4142 \pm 114	12 \pm 72	0.674
57478.3208	1478	4797 \pm 191	4592 \pm 146	147 \pm 90	0.719
57494.0163	1399	3943 \pm 176	4142 \pm 127	-6 \pm 181	0.541
57495.0476	1202	5148 \pm 228	5524 \pm 137	0 \pm 105	0.252
57500.1136	1726	5036 \pm 154	5294 \pm 99	-62 \pm 60	0.745
57505.2651	1329	5040 \pm 241	5478 \pm 138	61 \pm 87	0.297
57530.1287	1336	5076 \pm 216	4048 \pm 253	14 \pm 91	0.441
57531.2140	1113	5849 \pm 330	5501 \pm 171	-252 \pm 111	0.189
57532.0571	1271	6654 \pm 240	6179 \pm 112	-29 \pm 88	0.770

observations was presented in detail in our previous work (e.g., Hubrig, Schöller, & Kholtygin 2014; Hubrig et al. 2017 and references therein).

The longitudinal magnetic field was measured in two ways: using the entire spectrum including all available lines, or using exclusively the hydrogen lines. Furthermore, we have carried out Monte Carlo bootstrapping tests. These are most often applied with the purpose of deriving robust estimates of standard errors. The measurement uncertainties obtained before and after the Monte Carlo bootstrapping tests were found to be in close agreement, indicating the absence of reduction flaws. The results of our magnetic field measurements, those for the entire spectrum or only the hydrogen lines are presented in Table 1, where we also include in the first row the information about the previous magnetic field measurement presented by Castro et al. (2017). The rotation phase presented in the last column of Table 1 was calculated assuming a period of 1.45031 d, which was determined from our period search described in Sect. 3.

3 PERIOD DETERMINATION FROM THE MAGNETIC DATA

The result of our frequency analysis based on the longitudinal magnetic field measurements presented in Table 1 and performed using a non-linear least squares fit to multiple harmonics utilizing the Levenberg-Marquardt method (Press et al. 1992) with an optional possibility of pre-whitening the trial harmonics is presented in Fig. 1. Since the results of the measurements using the whole spectrum or exclusively the hydrogen lines are rather similar, the frequency analysis was performed using both, the measurements on the entire spectrum and on the hydrogen lines. To detect the most probable period, we calculated the frequency spectrum and for each

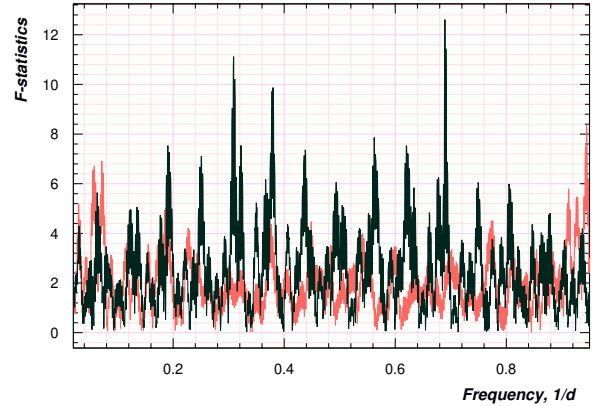


Figure 1. Frequency periodogram (in d^{-1}) for the longitudinal magnetic field measurements of CPD -62° 2124 using the entire spectrum and only the hydrogen lines. The window function is indicated by the red color.

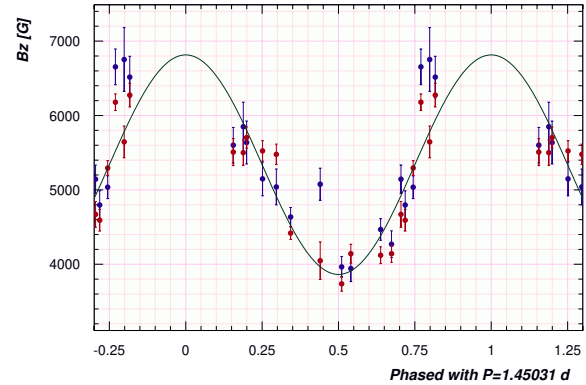


Figure 2. Longitudinal magnetic field variation of CPD -62° 2124 phased with the 1.45031 d period. Measurements of the magnetic field using the entire spectrum are presented by red circles, and those using hydrogen lines by blue circles. The solid line represents a fit to the data with a mean value for the magnetic field of $\langle B_z \rangle = 5339 \pm 87 \text{ G}$, an amplitude of $A_{(B_z)} = 1475 \pm 148 \text{ G}$, and a reduced χ^2 value of 2.7. For the presented fit, we assume a zero phase corresponding to a positive field extremum at MJD57300.3407.

trial frequency we performed a statistical F-test of the null hypothesis for the absence of periodicity (Seber 1977). The resulting F-statistics can be thought of as the total sum including covariances of the ratio of harmonic amplitudes to their standard deviations, i.e. a signal-to-noise ratio. The highest peak in the periodogram not coinciding with the window function corresponds to a period of $1.45031 \pm 0.00002 \text{ d}$.

In Fig. 2, we present all measurements, those using the entire spectrum and those using only the hydrogen lines, phased with the rotation period and the best sinusoidal fit calculated for these measurements. The largest gap in the phase coverage occurs in the phase range between 0.817 and 0.156. From the sinusoidal fit to our data, we obtain a mean value for the variable longitudinal magnetic field $\langle B_z \rangle = 5339 \pm 87 \text{ G}$ and an amplitude of the field variation $A_{(B_z)} = 1475 \pm 148 \text{ G}$. For the presented fit, we assume a zero phase corresponding to the field maximum at MJD57300.3407 \pm 0.0187. At phase 0.441, close to the magnetic field minimum, the measurement of the magnetic field using only the hydrogen lines, $\langle B_z \rangle_{\text{hyd}} = 5076 \text{ G}$, does not fall close to the

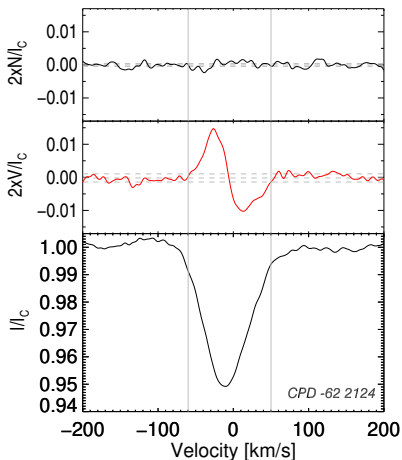


Figure 3. The Stokes I , V , and N LSD profiles of CPD $-62^\circ 2124$ obtained by the Potsdam group delivering $\langle B_z \rangle = 3.5 \pm 0.1$ kG.

magnetic field curve, unlike the magnetic field determined using the entire spectrum, $\langle B_z \rangle_{\text{all}} = 4048$ G. We currently do not have any explanation for the presence of this deviation in the measurements.

The simplest model for a magnetic field geometry is based on the assumption that the studied stars are oblique rotators, i.e., their magnetic field can be approximated by a dipole with its magnetic axis inclined to the rotation axis. For CPD $-62^\circ 2124$ Castro et al. (2017) determined the atmospheric parameters $T_{\text{eff}} = 23650$ K and $\log g = 3.95$, and measured the projected rotational velocity $v \sin i = 35 \pm 5$ km s $^{-1}$. Their comparison with stellar evolutionary tracks published by Ekstroem et al. (2012), and Brott et al. (2011) yielded the stellar radii $R = 5.8 \pm 0.9 R_\odot$ and $R = 5.05 \pm 0.76 R_\odot$, respectively. Using $P_{\text{rot}} = 1.45031 \pm 0.00002$ d and the estimate of the stellar radius $R = 5.8 \pm 0.9 R_\odot$, we obtain $v_{\text{eq}} = 202 \pm 31$ km s $^{-1}$ and an inclination angle of the stellar rotation axis to the line of sight $i = 10 \pm 2^\circ$. From the variation of the phase curve for the field measurements with a mean of $\langle B_z \rangle = 5339 \pm 87$ G and an amplitude of $A_{\langle B_z \rangle} = 1475 \pm 148$ G, we calculate $\langle B_z \rangle^{\text{min}} = 3864 \pm 172$ G and $\langle B_z \rangle^{\text{max}} = 6815 \pm 172$ G. Using the definition by Preston (1967)

$$r = \frac{\langle B_z \rangle^{\text{min}}}{\langle B_z \rangle^{\text{max}}} = \frac{\cos \beta \cos i - \sin \beta \sin i}{\cos \beta \cos i + \sin \beta \sin i}, \quad (1)$$

we find $r = 0.567 \pm 0.035$ and finally following

$$\beta = \arctan \left[\left(\frac{1-r}{1+r} \right) \cot i \right], \quad (2)$$

we calculate the magnetic obliquity angle $\beta = 58 \pm 6^\circ$. Assuming a limb-darkening coefficient of 0.3, typical for the $T_{\text{eff}} = 23650$ K (Castro et al. 2017), we estimate a dipole strength of 35.7 ± 4.4 kG using the model by Stibbs (1950). On the other hand, using the estimate of the stellar radius $R = 5.05 \pm 0.76 R_\odot$, we obtain $v_{\text{eq}} = 176 \pm 27$ km s $^{-1}$ and an inclination angle of the stellar rotation axis to the line of sight $i = 11 \pm 2^\circ$. For these parameters we calculate the magnetic obliquity angle $\beta = 54 \pm 6^\circ$ and estimate a dipole strength of 32.5 ± 3.5 kG. The obtained results for extremely large dipole magnetic field strengths place CPD $-62^\circ 2124$ as a record holder among the upper main-sequence early-B type stars with known magnetic fields.

The only available high-resolution spectropolarimetric observation of CPD $-62^\circ 2124$ was obtained with HARPS in the framework of the ESO Large Programme granted to the ‘‘B field in OB

stars’’ (BOB) collaboration (Morel et al. 2014) and corresponds to the phase 0.612, which is close to the observed longitudinal magnetic field minimum in the phase curve presented in Fig. 2. These HARPS data were acquired at a rather low signal-to-noise ratio of ~ 70 and were independently analysed by the Bonn and Potsdam groups (Castro et al. 2017). While the spectrum extraction is carried out in Bonn with their own routines, the analysis of the Potsdam group is based on two-dimensional spectra extracted using the ESO HARPS pipeline. Using the least-squares deconvolution technique (LSD; Donati et al. 1997) the Bonn group obtained a $\langle B_z \rangle$ of about 5.2 kG. However, applying the same technique and using the same list of lines for the measurements, the Potsdam group detected a $\langle B_z \rangle$ of about 3.5 kG. The LSD measurement obtained by the Potsdam group is presented in Fig. 3. Considering the phased FORS 2 magnetic field measurements presented in Fig. 2, a value of 3.5 kG appears to fit the phased curve better than a value of 5.2 kG.

Since CPD $-62^\circ 2124$ already finished a fractional main-sequence lifetime of about 60% and is already passing the β Cep instability strip, we checked the stability of the spectral lines in the Stokes I spectra over the full sequences of sub-exposures obtained on a time scale of minutes. Along with different radial velocity shifts of lines belonging to different elements, we also detect distinct changes in line profiles taking place on time-scales corresponding to the duration of the sub-exposure sequences for individual observations. In Fig. 4 we present the behaviour of line profiles in individual spectral lines belonging to carbon, silicon, and helium. The time difference between individual subexposures is between 15 and 19 min. Since with the current data we cannot decide on the periodicity of the detected variability, which is expected to be caused by the presence of β Cep-like pulsations, future observations should focus on a careful search for periodicity and the identification of pulsation modes. Due to the presence of the huge magnetic field in the atmosphere of this star, it presents the best candidate to test the impact of the magnetic field on internal mixing including core overshooting and internal rotation.

4 SPECTRAL VARIABILITY

Since magnetic early B-type stars usually exhibit spectral variability with the rotation period, we studied the variability of several spectral lines. Due to the rather low FORS 2 spectral resolution, we were only able to carry out a variability study using the strongest lines belonging to the elements hydrogen, helium, carbon, nitrogen, oxygen, aluminum, and silicon. In Figs. 5 and 6, we present the overlotted profiles of a few selected lines, H δ , H γ , H β , He I 4388, He I 4471, He I 5876, C II 4267, C III 4650, N II 4631, O II 4642, O II 4662, Al III 4529, Si III 4553, Si III 4568, and Si III 4575, the differences between the individual and average profiles, and the temporal behaviour of these differences in differential dynamic plots.

The appearance of differential dynamic plots is similar for all studied elements apart from helium. In the phase ranges 0.2-0.3 and 0.7-0.8 the hydrogen and the metal lines are redshifted while in the phase range between 0.3 and 0.7 in the vicinity of the minimum longitudinal magnetic field extremum the lines of these elements are on average blueshifted. The behaviour of the He I lines is clearly different, yet difficult to interpret, displaying a chessboard-like pattern. Also the analysis of the equivalent widths (EWs) variability for all lines, presented in Fig. 7, indicates the presence of an inhomogeneous element distribution: all elements, apart from helium, show an increase of their EWs towards the phase where the minimum longitudinal magnetic field extremum is observed. The in-

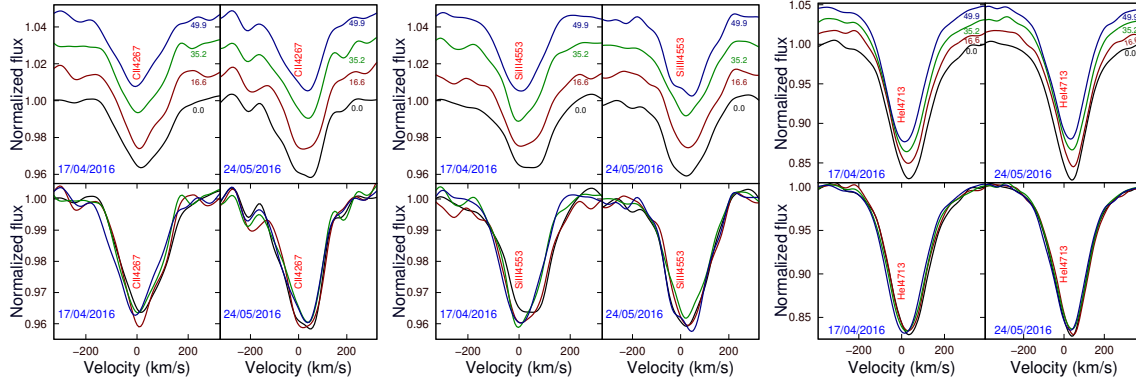


Figure 4. The behaviour of C II 4267, Si III 4553, and He I 4713 (from left to right) in the FORS2 spectra in each individual subexposure belonging to observations on two different epochs. For each epoch, in the upper row, we present the line profiles shifted in vertical direction for best visibility. The time difference (in minutes) between the subexposure and the start of observations is given close to each profile. The lower row shows all profiles overlapped.

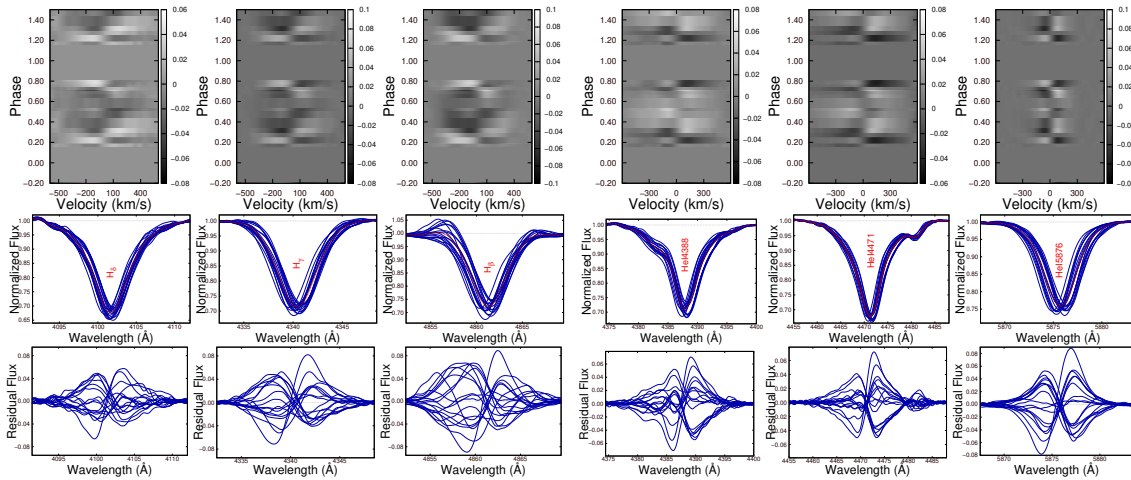


Figure 5. Variability of H δ , H γ , H β , He I 4388, He I 4471, and He I 5876 (from left to right) in the FORS2 spectra of CPD -62° 2124 over the rotational cycle. The middle and lower panels show the overlapped profiles and the differences between the individual and the average (red) line profiles. The upper panel presents the temporal behaviour of these differences.

tensity of the He lines decreases in the same phase range. The error bars of all presented EW measurements are of the order of the symbol size. Similar to our recent study of the behaviour of the H β line in the rigidly rotating magnetosphere star HD 345439 (Hubrig et al. 2017), the H β emission wings in CPD -62° 2124 show a slight asymmetry. The emission in the blue wing becomes stronger in the phase ranges 0.2–0.3 and 0.7–0.8, while a weaker emission in the red wing appears in the phase range 0.3–0.4 and around the phase 0.7.

5 DISCUSSION

Our spectropolarimetric monitoring of CPD -62° 2124 using FORS2 at the VLT reveals the presence of a huge magnetic field with a polar strength B_d between 32.5 and 35.7 kG, depending on the assumed stellar radius. Among the so far studied magnetic Ap stars, only Babcock’s star (HD 215441) possesses a similarly strong magnetic field with the field modulus changing from 32 to 35 kG (Babcock 1960; Preston 1969). No massive early-B type star is known to exhibit such a huge magnetic field strength as estimated in CPD -62° 2124. Remarkably, this strongly magnetic star,

although being in an advanced evolutionary state and having finished approximately 60% of its main-sequence life, rotates fast with $v_{\text{eq}} \geq 176 \pm 27 \text{ km s}^{-1}$ and has a short rotation period of $1.45031 \pm 0.00002 \text{ d}$. Only a small fraction of magnetic early-B type stars show such a high rotation rate (e.g. Hubrig et al. 2017) while for the majority of the magnetic Ap and Bp stars it is expected that magnetic braking slows stellar rotation (e.g., Mathys 2004). On the other hand, the study of strongly magnetic stars by Hubrig et al. (2000) did not show any correlations between the rotation period and the fraction of the main-sequence lifetime completed. Clearly, fast rotating strongly magnetic early-B type stars in an advanced evolutionary state are of special interest for our understanding of the evolution of the angular momentum and spindown timescales in the presence of a magnetic field.

Modelling of the magnetic field geometry of CPD -62° 2124 indicates the presence of an organized magnetic field with an important dipole component. Our study of the spectral variability showed the presence of significant chemical abundance variations across the stellar photosphere with the helium abundance decreasing towards the longitudinal magnetic field minimum and an increase of the abundances of other elements studied in the same phases. Future high-resolution high signal-to-noise spectropolari-

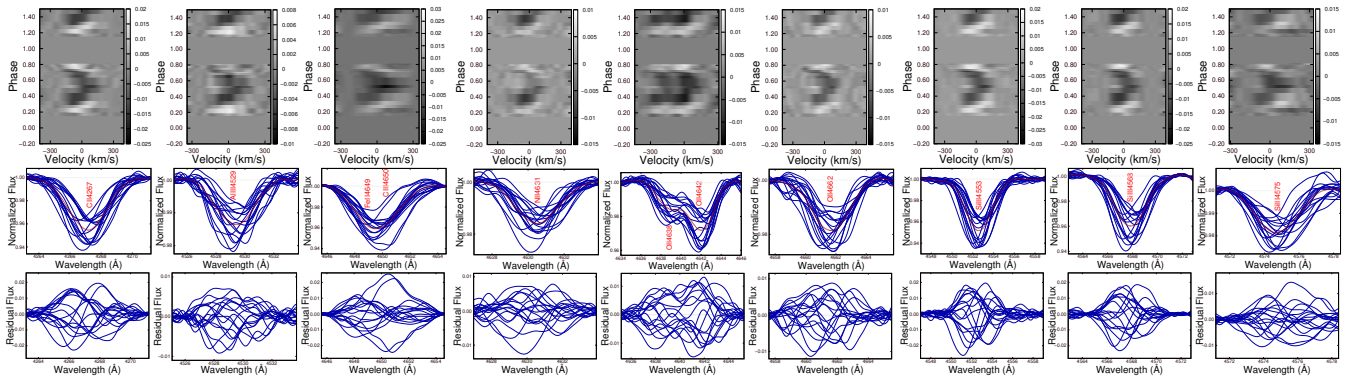


Figure 6. Same as in Fig. 5, but for the lines C II 4267, Al III 4529, C III 4650, N II 4631, O II II 4642, O II 4662, Si III 4553, Si III 4568, and Si III 4575 (from left to right).

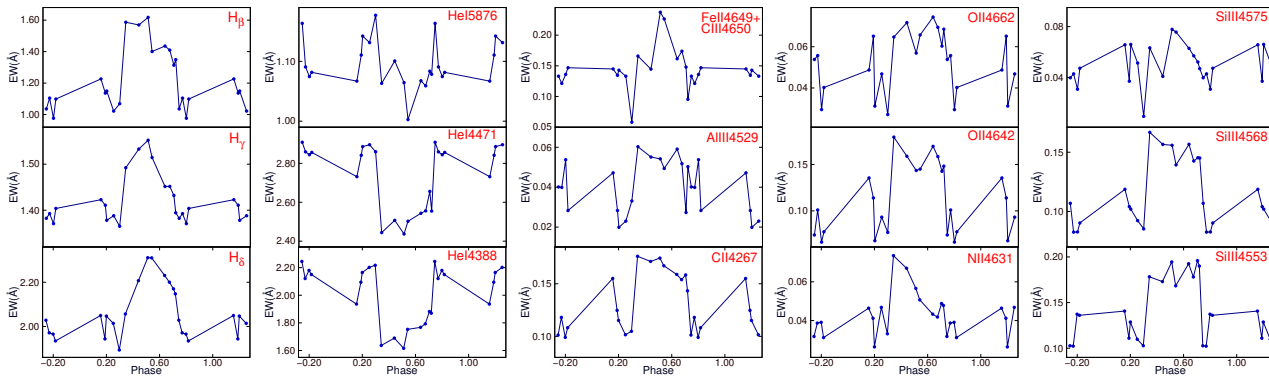


Figure 7. Variability of EWs of lines belonging to different elements in FORS 2 spectra of CPD $-62^\circ 2124$ obtained at seventeen different rotational phases.

metric observations will be worthwhile to determine the surface distribution of different elements. We also discovered pulsational variability most likely caused by β Cep-like pulsations. A future detailed seismic study of CPD $-62^\circ 2124$ will be of great importance to constrain physical processes in magnetic stars and to test the impact of the magnetic field on the internal mixing processes. As this star is rather bright and has relatively low projected rotational velocity, it appears to be an excellent candidate also for future high-resolution polarimetric studies to study various atmospheric effects that interact with a strong magnetic field.

ACKNOWLEDGMENTS

Based on observations made with ESO Telescopes at the La Silla Paranal Observatory under programme ID 097.D-0428(A). AK acknowledges financial support from RFBR grant 16-02-00604A.

REFERENCES

- Appenzeller I., et al., 1998, *The Messenger*, 94, 1
 Babcock H. W., 1980, *ApJ*, 132, 521
 Brott I., et al., 2011, *A&A*, 530, A115
 Castro N., et al., 2017, *A&A*, 597, L6
 Donati J.-F., Semel M., Carter B. D., Rees D. E., Collier Cameron A., 1997, *MNRAS*, 291, 658
 Ekström S., et al., 2012, *A&A*, 537, A146
 Hubrig S., North P., Mathys G., 2000, *ApJ*, 539, 352

- Hubrig S., Schöller M., Kholtygin A. F., 2014, *MNRAS*, 440, L6
 Hubrig S., Kholtygin A. F., Schöller M., Ilyin I., 2017, *MNRAS*, *in print*
 Mathys G., 2004, *Proc. of IAU Symp.* 215, p. 270
 Morel T., et al., 2014, *The Messenger*, 157, 27
 Press W. H., Teukolsky S. A., Vetterling W. T., Flannery B. P., 1992, *Numerical Recipes*, 2nd edn. Cambridge Univ. Press, Cambridge
 Preston G. W., 1967, *ApJ*, 150, 547
 Preston G. W., 1969, *ApJ*, 156, 967
 Seber G. A. F., 1977, *Linear Regression Analysis* (New York: Wiley)
 Snik F, et al., 2011, in *Solar Polarization 6*, ASP Conf. Ser., 437, 237
 Stibbs D. W. N., 1950, *MNRAS*, 110, 395